



# Screened electrostatic interactions between clay platelets

D. G. ROWAN<sup>1\*</sup>, J.-P. HANSEN<sup>1</sup> and E. TRIZAC<sup>2</sup>

<sup>1</sup> Department of Chemistry, University of Cambridge, Lensfield Road, Cambridge CB2 1EW, UK

<sup>2</sup> Laboratoire de Physique Theorique (UMR 8627), Bat. 211, Universite Paris-Sud, 91405 Orsay Cedex, France

(Received 21 March 2000; accepted 17 April 2000)

An effective pair potential for systems of uniformly charged lamellar colloids in the presence of an electrolytic solution of microscopic co- and counterions is derived. The charge distribution on the discs is expressed as a collection of multipole moments, and the tensors which determine the interactions between these multipoles are derived from a screened Coulomb potential. Unlike previous theoretical studies of such systems, the interaction energy may now be expressed for discs at arbitrary mutual orientation. The potential is shown to be exactly equivalent to the use of linearized Poisson–Boltzmann theory.

## 1. Introduction

While the mesostructure, stability and phase behaviour of charge-stabilized dispersions of spherical colloidal particles are by now reasonably well understood, both experimentally and theoretically [1–3], the picture is much less clear in the case of lamellar colloids, of which clay dispersions are a pre-eminent example [4]. This is due partly to the high degree of polydispersity, the irregular shapes, and the extreme anisotropy of the thin lamellar particles of naturally occurring clay suspensions. Such complications render an unambiguous interpretation of experimental data, e.g. from small angle X-ray or neutron diffraction measurements, very difficult, while posing a practically insurmountable challenge to the theoretician attempting a statistical mechanics description. Even for the widely studied synthetic model system of laponite, made up of nearly monodisperse, disc-shaped platelets, there is no consensus among experimentalists as to the structure, gelling behaviour and rheology of semi-dilute suspensions [5–9], while attempts at a theoretical description, or simulations of this model system are in their infancy [10, 11]. The main reason for the latter state of affairs is that a realistic model for the effective interaction between a pair of arbitrarily oriented charged circular platelets, generalizing the isotropic DLVO potential [1] between spherical colloids, is not available. Only in the simplest case of two coaxial, uniformly charged discs, has a screened Coulomb interaction been worked out

within linear [12] and nonlinear [13] Poisson–Boltzmann (PB) theory.

The molecular dynamics (MD) simulations of [11] were based on a site–site interaction model, generalizing the ‘Yukawa segment’ representation used earlier to simulate suspensions of charged rods [14]. Within such a representation the charge distribution on a rod or a platelet is discretized into  $\nu$  interaction sites, each carrying a fraction  $1/\nu$  of the total charge; sites on different particles interact via a screened Coulomb potential. This Yukawa segment model is very computationally intensive, since the total interaction between two particles involves  $\nu^2$  contributions. It also carries a degree of arbitrariness in the choice of the number of sites  $\nu$ , which for practical reasons must be taken to be much smaller than the number of elementary surface charges (typically  $10^3$  for laponite) carried by individual platelets.

This paper examines the continuous version of the Yukawa segment model, and derives a multipolar expansion of the effective, screened Coulomb interaction between two uniformly charged platelets of arbitrary relative orientations. The resulting anisotropic effective pair potential is shown to be accurate for centre-to-centre distances larger than the radius of the platelets, and should hence provide a useful tool for theoretical investigations of the structure and sol–gel transition in semi-dilute clay dispersions.

## 2. The Yukawa segment model

Consider a suspension of  $N_p$  infinitely thin circular platelets per unit volume, of radius  $a$ , and carrying a uniform surface charge density  $\sigma = Ze/\pi a^2$ , where  $Ze$

\* Author for correspondence. e-mail: rowan@theor.ch.cam.ac.uk

( $< 0$ ) is the total charge on a platelet. The platelets, together with microscopic co- and counterions, are suspended in water. Since the present study focuses on mesoscopic lengthscales, of the order of  $a$  (typically  $a \simeq 15\text{nm}$  for Laponite), one may neglect the molecular nature of water, which will be regarded as a continuum of dielectric constant  $\varepsilon$ . Within linearized PB theory, the effective interactions between platelets are always pairwise additive [15], and the screening of electrostatic interactions by the co- and counterions is uniquely characterized by the Debye screening length:

$$\lambda_D = \frac{1}{\kappa} = \left( \sum_{\alpha} \frac{n_{\alpha} z_{\alpha}^2 e^2}{\varepsilon_0 \varepsilon k_B T} \right)^{-1/2}, \quad (1)$$

where the sum is over all microion species,  $n_{\alpha}$  and  $z_{\alpha}$  are the concentration (number density) and valence of ions of species  $\alpha$ , and  $\varepsilon_0$  is the permittivity of free space. Building on the linearity of the theory, the Yukawa segment model assumes that each infinitesimal area  $ds$  (or ‘segment’) on a uniformly charged disc generates a screened Coulomb potential

$$\phi(r) = \frac{\sigma ds}{4\pi\varepsilon_0\varepsilon r} e^{-\kappa r}. \quad (2)$$

The corresponding pair potential between two infinitesimal areas  $ds$  (around  $\mathbf{r}$ ) and  $ds'$  (around  $\mathbf{r}'$ ) on two discs is then

$$v(|\mathbf{r} - \mathbf{r}'|) = \frac{\sigma^2 ds ds'}{4\pi\varepsilon_0\varepsilon |\mathbf{r} - \mathbf{r}'|} e^{-\kappa|\mathbf{r} - \mathbf{r}'|}, \quad (3)$$

and the total pair interaction between the discs is obtained by integrating expression (3) over the surfaces of the two discs. However, for arbitrary orientations of the discs, this leads to intractable expressions involving multiple integrals.

Instead, by analogy with electrostatic interactions between extended charge distributions, a systematic multipolar expansion of the screened Coulombic interaction will be sought. The derivation of such an expansion requires some care, because the basic screened Coulomb potential (2) does not satisfy Poisson’s equation, except in the bare Coulomb limit, where  $\kappa \rightarrow 0$ .

### 3. The potential around a single plate

To get a feeling for a multipolar expansion involving screened, rather than bare, Coulomb interactions, consider first the potential due to a uniformly charged disc, along the axis of the disc. Using cylindrical coordinates, with the  $z$  coordinate along the axis of the disc (cf. figure 1), the screened potential along that axis (i.e. for a radial coordinate  $\rho = 0$ ) is simply

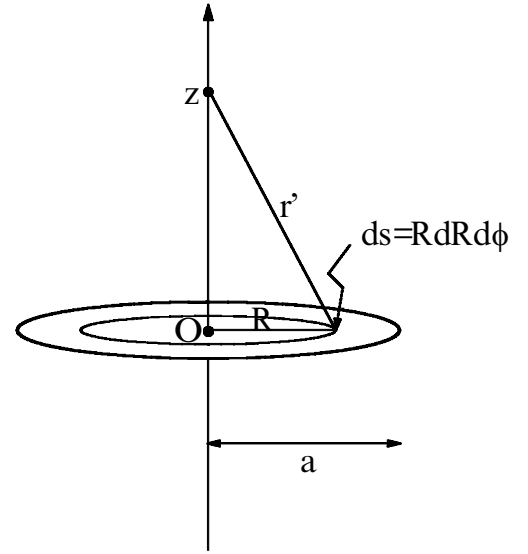


Figure 1. Integration over the surface of a disc.

$$\begin{aligned} \Psi(\rho = 0, z) &= \frac{2\pi\sigma}{4\pi\varepsilon_0\varepsilon} \int_0^a \frac{e^{-\kappa\sqrt{R^2+z^2}}}{\sqrt{z^2+R^2}} R dR \\ &= \frac{\sigma e^{-\kappa|z|}}{2\varepsilon_0\varepsilon\kappa} [1 - e^{-\kappa|z|} [\sqrt{1+(\frac{a}{z})^2} - 1]], \end{aligned} \quad (4)$$

which is easily expanded in powers of  $(a/z)$  according to

$$\Psi(\rho = 0, z) = \frac{Ze}{4\pi\varepsilon_0\varepsilon} e^{-\kappa|z|} \sum_{n=0}^{\infty} [A_n + K_n] \left(\frac{1}{|z|}\right)^{n+1}, \quad (5)$$

where the coefficients  $A_n$  and  $K_n$  are listed in table 1.

Several points are to be noted about this expansion. First, the corresponding expansion for the bare Coulomb potential is correctly retrieved by taking the limit  $\kappa \rightarrow 0$ ; this amounts to setting all  $K_n = 0$  in equation (5), leaving only odd powers of  $1/z$  in the expansion, since all odd coefficients  $A_n$  vanish. This is an obvious consequence of the space reflection symmetry of the uniform charge distribution on a disc, which implies that only even multipole moments exist. However, for the screened Coulomb potential, terms with even powers of  $1/z$  appear in the expansion, which would correspond to odd multipoles (dipole, etc.) in the bare Coulomb case.

The second remark is that expansion (5) also follows from the exact potential due to a uniformly charged disc, and its associated electric double-layer of co- and counter ions, as calculated within linearized PB theory [16], namely

$$\Psi(\rho, z) = \frac{2Ze}{a\varepsilon_0\varepsilon} \int_0^{\infty} J_1(ka) J_0(k\rho) \frac{e^{-|z|\sqrt{k^2+\kappa^2}}}{\sqrt{k^2+\kappa^2}} dk. \quad (6)$$

Table 1. Coefficients appearing in the series expansion of the electrostatic potential along the  $z$  axis (equation (5)):  $C_{1/2}^n$  is the coefficient of the term of order  $x^n$  in the binomial expansion of  $(1+x)^{1/2}$ .

$n$	$A_n$	$K_n$
0	+1	0
1	0	$-\frac{\kappa a^2}{4}$
2	$-\frac{a^2}{4}$	$+\frac{\kappa^2 a^4}{24}$
3	0	$+\frac{\kappa a^4}{8} - \frac{\kappa^3 a^6}{192}$
4	$\frac{+a^4}{8}$	$-\frac{\kappa^2 a^6}{32} + \frac{\kappa^2 a^8}{1920}$
5	0	$-\frac{5\kappa a^6}{64} + \frac{\kappa^3 a^8}{192} - \frac{\kappa^2 a^{10}}{23040}$
$\vdots$	$\vdots$	$\vdots$
$n$ even	$2a^n C_{1/2}^{(n/2)+1}$	$\vdots$
$n$ odd	0	$\vdots$

This agreement between the expansion in equation (5) and the expansion of equation (6) for  $\rho = 0$  is an illustration of the exact equivalence between the Yukawa segment model and a full linearized PB calculation of the effective potential generated by a charged particle of any shape and its associated electric double layer.

The final point concerns the generalization of expansion (5) away from the  $z$  axis, i.e. for  $\rho \neq 0$ . In the bare Coulomb case ( $\kappa = 0$ ), the coefficients  $A_n$  in table 1 may be immediately carried over to spherical polar coordinates  $(r, \theta, \phi)$  to write down an expansion of the potential due to a uniformly charged disc in even Legendre polynomials (the potential is independent of the azimuthal angle  $\phi$ ):

$$\Psi(r, \theta) = \frac{Ze}{4\pi\epsilon_0\epsilon} \sum_{n=0; \text{even}}^{\infty} A_n \frac{1}{r^{n+1}} P_n(\cos \theta). \quad (7)$$

However, the presence of the exponential screening factor in expansion (5) prevents a similar straightforward generalization to off-axis conditions in the screened Coulomb case ( $\kappa \neq 0$ ). For this reason the multipolar expansion must be re-examined more carefully for the Yukawa segment model.

#### 4. Screened multipolar expansion

The multipolar expansion of the total potential  $\Psi(\mathbf{r})$  due to a uniformly charged disc, with each infinitesimal surface element generating the screened potential (2) (Yukawa segment model), may be derived along lines nearly identical to the classic calculation for unscreened charge distributions [17]. Clearly

$$\Psi(\mathbf{r}) = \int_S \phi(|\mathbf{r} - \mathbf{s}|) ds \quad (8)$$

where the integral is over the surface  $S$  of the disc. The potential  $\phi$  may now be expanded as a Taylor series about the centre of the disc ( $\mathbf{s} = \mathbf{0}$ ), i.e.

$$\Psi(\mathbf{r}) = \sigma \int_S ds \left\{ \phi(r) - \sum_{\alpha} s_{\alpha} \nabla_{\alpha} \phi(r) + \frac{1}{2!} \sum_{\alpha\beta} s_{\alpha} s_{\beta} \nabla_{\alpha} \nabla_{\beta} \phi(r) + \dots \right\}, \quad (9)$$

where the sums are over all three Cartesian coordinates of the vector  $\mathbf{s} \in S$ . All odd terms (e.g. the dipolar term) vanish by symmetry. This leaves only the even terms:

$$\Psi(\mathbf{r}) = \Psi_Z(r) + \Psi_Q(\mathbf{r}) + \Psi_{\Phi}(\mathbf{r}) + \dots, \quad (10)$$

involving the total charge  $Ze$  of the disc, its quadrupole tensor  $\mathbf{Q}$ , its hexadecapole tensor  $\Phi$ , etc.,

$$\begin{aligned} \Psi_Z(r) &= Ze T^{\kappa}(r), \\ \Psi_Q(\mathbf{r}) &= \frac{e}{2!} Q_{\alpha\beta} T^{\kappa}_{\alpha\beta}(\mathbf{r}), \\ \Psi_{\Phi}(\mathbf{r}) &= \frac{e}{4!} \Phi_{\alpha\beta\gamma\delta} T^{\kappa}_{\alpha\beta\gamma\delta}(\mathbf{r}), \end{aligned} \quad (11)$$

where the Einstein convention of summation over repeated indices has been adopted. The tensors  $T^{\kappa}$  are:

$$T^{\kappa}_{\alpha\beta\gamma\dots} = \nabla_{\alpha} \nabla_{\beta} \nabla_{\gamma} \dots \left( \frac{1}{4\pi\epsilon_0\epsilon} \frac{e^{-\kappa r}}{r} \right), \quad (12)$$

while the  $Q_{\alpha\beta}, \Phi_{\alpha\beta\gamma\delta}$  are the Cartesian components of the 2nd rank quadrupolar and 4th rank hexadecapolar tensors. For a uniformly charged disc the quadrupolar tensor is given (in a frame where the  $z$  coordinate is along the axis of the disc) by

$$\begin{aligned} \mathbf{Q} &= \frac{\sigma}{e} \int_S s ds \\ &= \begin{pmatrix} -Q & 0 & 0 \\ 0 & -Q & 0 \\ 0 & 0 & 0 \end{pmatrix}, \end{aligned} \quad (13)$$

where  $Q = -Za^2/4$ . Note that, contrary to the bare Coulomb case,  $\mathbf{Q}$  cannot be chosen traceless in the screened case, because the tensors  $T^{\kappa}_{\alpha\beta\dots}$  are themselves

not traceless. The Cartesian components of the 4th rank hexadecapole moment are defined by

$$\Phi_{\alpha\beta\gamma\delta} = \frac{\sigma}{e} \int_S s_\alpha s_\beta s_\gamma s_\delta d\mathbf{s}. \quad (14)$$

For a disc, choosing the  $z$  coordinate along its axis, the only nonzero components  $\alpha\beta\gamma\delta$  are the two diagonal components  $\Phi_{xxxx}$  and  $\Phi_{yyyy}$  and those in which  $x$  and  $y$  both appear twice. Explicitly,

$$\begin{aligned} \Phi_{xxxx} &= \Phi_{yyyy} = \frac{Za^4}{8} \equiv \Phi \\ \Phi_{xxyy} &= \Phi_{xyxy} = \dots = \frac{Za^4}{24} \equiv \frac{\Phi}{3}. \end{aligned} \quad (15)$$

The calculation of the tensors  $T_{\alpha\beta\gamma\dots}^\kappa$  is considerably lengthier for the screened than for the bare Coulomb interaction. Some details are given in appendix A.

In spherical coordinates, the total potential due to the uniformly charged disc, up to hexadecapolar order, may finally be written as:

$$\begin{aligned} \Psi(r, \theta) &= \frac{e}{4\pi\epsilon_0\epsilon} e^{-\kappa r} \left\{ \frac{1}{r} \left[ Z + \frac{Q}{2} \kappa^2 (\cos^2 \theta - 1) \right. \right. \\ &+ \frac{\Phi}{24} \kappa^4 \sin^4 \theta \left. \right] + \frac{1}{r^2} \left[ \frac{Q}{2} \kappa (3 \cos^2 \theta - 1) \right. \\ &- \frac{\Phi}{3} \kappa^3 \left( \sin^2 \theta - \frac{5}{32} \sin^4 \theta \right) \left. \right] \\ &+ \frac{1}{r^3} \left[ \frac{Q}{2} (3 \cos^2 \theta - 1) \right. \\ &+ \frac{\Phi}{3} \kappa^2 \left( 1 - 6 \sin^2 \theta + \frac{45}{8} \sin^4 \theta \right) \left. \right] \\ &+ \frac{1}{r^4} \left[ \frac{\Phi}{8} \kappa (35 \cos^4 \theta - 30 \cos^2 \theta + 3) \right. \\ &\left. \left. + \frac{1}{r^5} \left[ \frac{\Phi}{8} (35 \cos^4 \theta - 30 \cos^2 \theta + 3) \right] \right\}. \end{aligned} \quad (16)$$

Returning to cylindrical coordinates, this expression reduces on the  $z$  axis to

$$\begin{aligned} \Psi(\rho=0, z) &= \frac{Ze}{4\pi\epsilon_0\epsilon} e^{-\kappa|z|} \left[ \frac{1}{z} - \frac{\kappa a^2}{4} \left( \frac{1}{z} \right)^2 \right. \\ &+ \left( \frac{\kappa^2 a^4}{24} - \frac{a^2}{4} \right) \left( \frac{1}{z} \right)^3 + \frac{\kappa a^4}{8} \left( \frac{1}{z} \right)^4 \\ &\left. + \frac{a^4}{8} \left( \frac{1}{z} \right)^5 \right], \end{aligned} \quad (17)$$

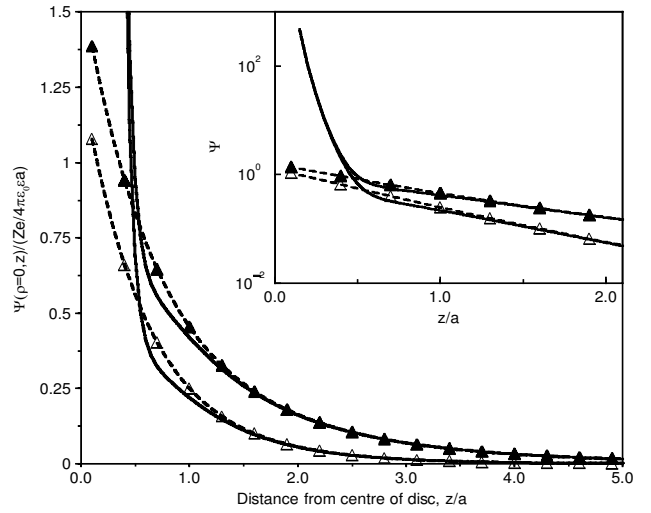


Figure 2. Electrostatic potential along the  $z$  axis: solid lines, multipolar expansion; dashed lines, linearized PB potential; and triangles, a numerical integration over a discretized charge distribution (Yukawa segment model); upper set of curves,  $\kappa a = 0.5$ ; lower set,  $\kappa a = 1.0$ . The divergence is highlighted in the logarithmic inset figure.

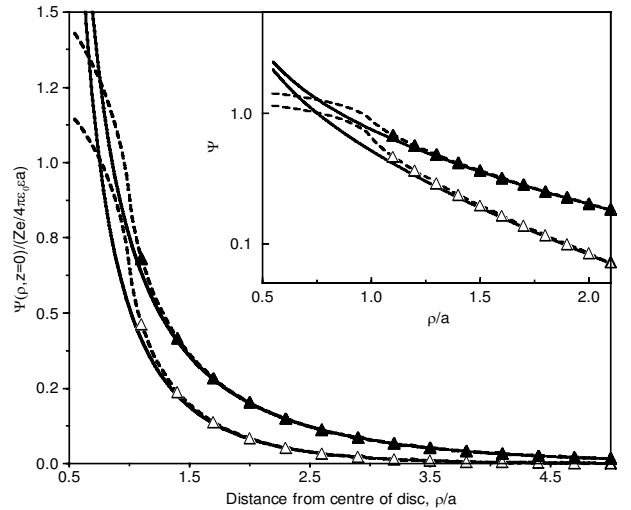


Figure 3. Electrostatic potential in the  $xy$  plane (symbols as in figure (2)) for  $\kappa a = 0.5$  and  $1.0$ .

which coincides with expansion (5), with coefficients given in table 1, up to order  $a^4$  (the higher powers of  $a$  in the coefficients of  $1/z^4$  and  $1/z^5$  corresponding to higher order multipole moments). To illustrate the convergence of the multipolar expansion of the potential to hexadecapolar order, in figures 2 and 3 the potential given by expression (16) is compared with the linearized PB potential of equation (6) and an explicit numerical integration over a discretized charge distribution (with  $\nu = 7841$  sites), both along the  $z$  axis and in the  $xy$  plane. The numerical integration was carried out to



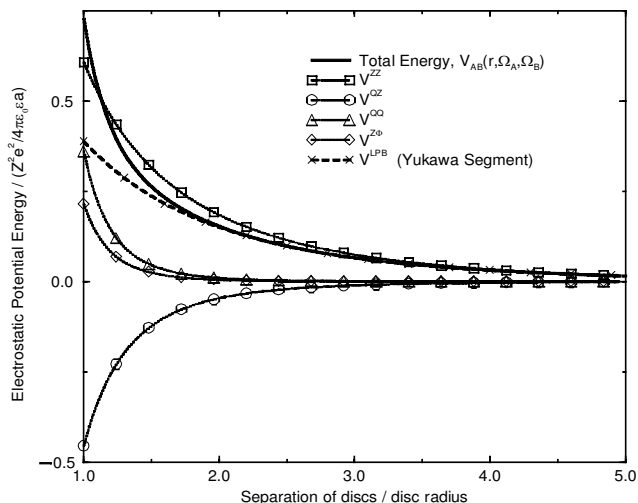


Figure 5. Contributions to the potential energy as a function of separation for two parallel coaxial plates ( $\theta_A = 0, \theta_B = 0, \Delta\phi = 0$ ), for inverse screening length  $\kappa = 0.5/a$ . The points plotted on the LPB curve (known in this geometry) correspond to a discretized Yukawa segment model calculation.

of the two discs;  $\Delta\phi$ , the difference in the azimuthal angles of the two discs; and  $\kappa$ , the inverse screening length determined by the co- and counterions. Rather than specialize to the physical parameters particular to laponite ( $Z \approx -1000$ ,  $a \approx 15$  nm), in the figures that follow, all distances will be scaled by the disc radius  $a$ , which provides a convenient length scale, and all energies by the bare Coulombic energy of two charges  $Ze$  a distance  $a$  apart, i.e. by  $Z^2 e^2 / 4\pi\epsilon_0 \epsilon a$ . Thus these results apply to the most general uniformly charged disc.

The case of two coaxial plates is illustrated in figure 5, where the various contributions to the energy  $V_{AB}$  are plotted as a function of the distance between the two plates. The exact result in this simple geometry is known within LPB theory [12], and used to test the convergence of the multipolar series. As expected, the charge–charge contribution (22) dominates for large spacings, but the contributions of the higher order terms become very significant for spacings less than the disc diameter,  $2a$ .

In figure 6 the energy is plotted as a function of the separation between two discs lying in the same plane, like two coins on a table. In this geometry all multipolar contributions are positive (repulsive), and the enhancement of the total energy over the charge–charge term is more pronounced. Included in this figure is the potential energy obtained by integrating over the Yukawa potential over two discretized site-charge distributions, where each disc has  $\nu = 7841$  point charges, each carrying charge  $Ze/\nu$ . The agreement of this calculation with the multipolar expansion is excellent, down to the dis-

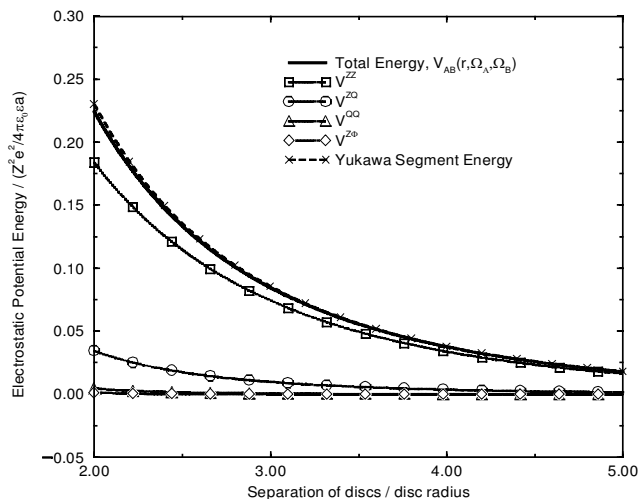


Figure 6. Contributions to the potential energy as a function of separation for two parallel coplanar plates ( $\theta_A = \pi/2, \theta_B = \pi/2, \Delta\phi = 0$ ), again for  $\kappa a = 0.5$ . The discretized Yukawa segment calculation has been included for comparison.

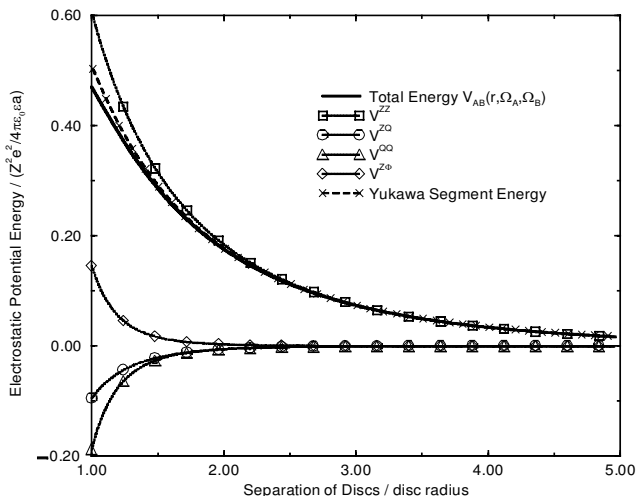


Figure 7. Contributions to the potential energy as a function of separation for two plates in T-shape configuration ( $\theta_A = 0, \theta_B = \pi/2, \Delta\phi = 0$ ) with  $\kappa a = 0.5$ . The discretized Yukawa segment calculation has been included for comparison.

tance of closest approach  $r = 2a$  below which point the discs intersect.

In figure 7 the energy is plotted as a function of the separation of two discs in a T-shaped configuration ( $\theta_A = 0, \theta_B = \pi/2$ ), a geometry favoured by the quadrupoles, as also observed in [10], where a purely quadrupolar disc model was studied. The agreement with the discretized Yukawa segment calculation is again excel-

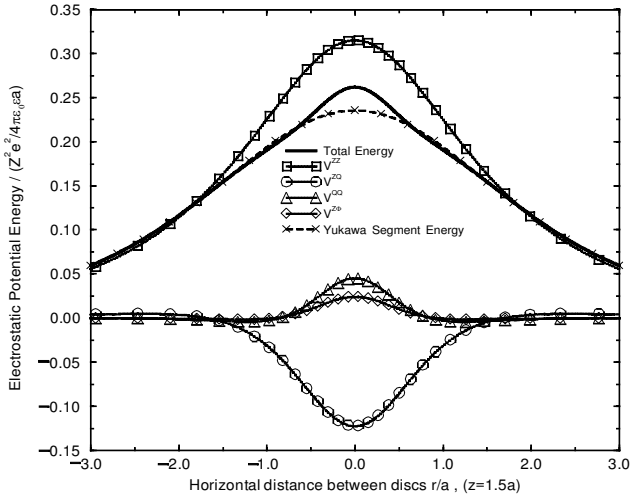


Figure 8. Contributions to the potential energy as a function of the horizontal separation  $r/a$ , for parallel plates with plate  $B$  fixed at an altitude of  $1.5a$  above plate  $A$  and  $\kappa a = 0.5$ . The discretized Yukawa segment calculation has been included for comparison.

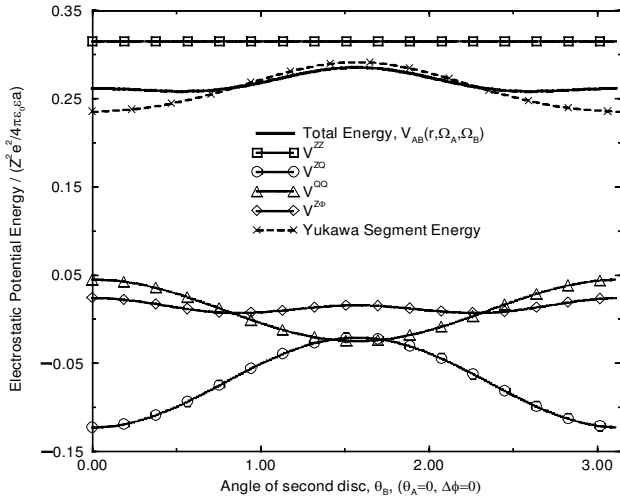


Figure 9. Contributions to the potential energy as a function of the angle  $\theta_B$  with  $\theta_A = 0$  for  $\kappa a = 0.5$ , and fixed centre-to-centre distance  $r = 1.5a$ . The discretized Yukawa segment calculation has been included for comparison.

lent, except at very close centre-to-centre separations, where the multipolar expansion is expected to collapse.

In figure 8 the behaviour of the pair potential is examined as one disc slides over the other at constant altitude ( $z = 1.5a$  in this plot), with the two discs parallel to each other. As expected the energy goes through a maximum at the distance of closest approach, but detailed structure is seen in the total energy, as each order of multipole–multipole interaction decays with differing power law behaviour. The agreement with the numerical Yukawa segment calculation is again good, except in

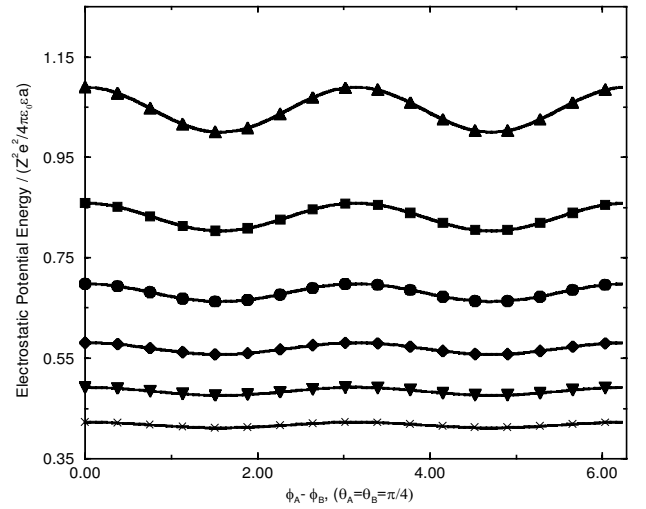


Figure 10. Dependence of the energy on the difference in azimuthal angle  $\Delta\phi$ , plotted for fixed  $\theta_A = \theta_B = \pi/4$  for disc separations  $r/a = 1.0, 1.1, 1.2, 1.3, 1.4$  and  $1.5$ , from top to bottom, for  $\kappa a = 0.5$ .

the region around closest approach, where the platelets are co-axial, and the greatest deviation is observed, as seen in figure 5. This deviation decreases significantly the greater the vertical separation of the platelets, and may be improved at close separation by the inclusion of higher order multipole moments.

In figure 9, the angular dependence of the potential is examined by varying the angle  $\theta_B$  at fixed centre-to-centre separation of  $r = 1.5a$  and  $\theta_A = 0$ . Obviously the charge–charge interaction is independent of relative orientation, but significant variation in all higher order interactions is observed. Notably, the quadrupole–quadrupole interaction is favoured when the discs are perpendicular to each other. The agreement with the computationally expensive numerical integration method is observed to be good, except when the discs are parallel, where the deviation is most noticeable, as observed and commented upon in figures 5 and 8.

Finally in figure 10 the dependence of the interaction on the azimuthal angles is probed, for disc separations in the range  $1 < r/a < 1.5$  for discs fixed at  $\theta_A = \theta_B = \pi/4$ . As noted in appendix B, the interaction energy depends only on the difference  $\Delta\phi = \phi_A - \phi_B$ . As the separation of the discs increases, the angular dependence of the pair potential is seen to diminish, and indeed at large separations disappears.

## 7. Conclusion

The familiar multipole moment expansion of the electrostatic interaction between two extended charge distributions have been generalized to the case where the interaction is linearly screened by co- and counterions of

an ionic solution in which the charged colloidal particles are dispersed. The case of uniformly charged, disc-like platelets, a model for the synthetic clay laponite, was specifically considered in this paper, but the Yukawa-segment model, and the corresponding multipolar expansion, may be extended to particles of any shape. For example, this procedure may be adapted readily to the case of uniformly charged rods, where symmetry again precludes multipole moments of odd order, by insertion of the relevant quadrupole and hexadecapole tensors for such a charge distribution. In the simplest case of spherical particles, the present treatment leads back to the familiar DLVO potential. For discs, the expansion, including up to quadrupole–quadrupole and charge–hexadecapole terms, yields interaction energies in good agreement with data for a discretized version of the Yukawa segment model, down to centre-to-centre distances of the order of the disc radius  $a$ , for all relative orientations of the two platelets which were investigated. As expected, the expansion breaks down at shorter distances, and yields rapidly divergent energies as  $r \rightarrow 0$ .

The effective pair potential defined by equation (21), and the explicit expressions in the appendices, should prove useful in statistical mechanics descriptions of semi-dilute clay dispersions, and of their sol–gel transition, provided suitable short range cutoffs are imposed. For computer simulations of more concentrated dispersions, an appropriate strategy would be to use a hybrid pair potential approach, interpolating between the multipolar expansion at large centre-to-centre distances, and a direct summation of the  $\nu^2$  screened Coulomb site–site interactions in a discretized version of the Yukawa segment model, similar to that used in [11], at short distances.

In order to determine the phase behaviour of dispersions of charged platelets, from direct calculations of the free energy of systems of platelets interacting via the multipolar effective pair potential derived in this paper, it is important to include a structure-independent ‘volume’ term in the free energy [18]. Such a volume term has been shown to play a crucial role in the determination of phase diagrams of suspensions of spherical charged colloidal particles, in the regime of very low concentration of added electrolyte [3, 19]. The exact form of the ‘volume’ term can be determined from a careful analysis of the density functional formulation of linearized PB theory [3, 15]. Such an analysis, which also provides a rigorous foundation of the Yukawa segment model [11], is under way.

The authors would like to thank H. Löwen and A. J. Stone for useful discussions, and gratefully acknowledge the support of the Franco-British Alliance Program,

Project No. PN 99.041. D.G.R. would like to thank the EPSRC for their continued support.

## Appendix A

### *Cartesian tensors for a screened Coulomb interaction*

The Cartesian tensors for a screened Coulomb interaction are defined (analogously to the bare Coulomb case) as derivatives of the potential, i.e.

$$T_{\alpha\beta\gamma}^{\kappa} = \nabla_{\alpha}\nabla_{\beta}\nabla_{\gamma}\left(\frac{1}{4\pi\epsilon_0\epsilon}\frac{e^{-\kappa r}}{r}\right) \quad (\text{A } 1)$$

Now, for any function  $f(r)$ , ( $f(r)$  being  $e^{-\kappa r}/r$  in the current work) the gradient  $\nabla_{\alpha}f(r) = f'(r)\nabla_{\alpha}r$ . For the bare Coulomb potential,  $f(r) = 1/r$ , and thus  $\nabla_{\alpha}(1/r) = -(1/r^2)\nabla_{\alpha}r \equiv T_{\alpha}^0$ . Combining these two simple results the gradient of a general function  $f(r)$  may be expressed in terms of the bare Coulomb tensor via  $\nabla_{\alpha}f(r) = -r^2f'(r)T_{\alpha}^0$ . Introducing the differential operator  $\mathcal{D}$ , defined by  $\mathcal{D}f(r) = -r^2f'(r)$ , this may furthermore be written as  $\nabla_{\alpha}f(r) = \mathcal{D}f(r)T_{\alpha}^0$ . Thus the set of successive interaction tensors for a screened Coulomb potential  $T^{\kappa}$  may be written, using the product rule of differentiation, as

$$\begin{aligned} T_{\alpha}^{\kappa} &= \nabla_{\alpha}f(r) = (\mathcal{D}^1f)T_{\alpha}^0, \\ T_{\alpha\beta}^{\kappa} &= \nabla_{\alpha}\nabla_{\beta}f(r) = (\mathcal{D}^2f)T_{\alpha}^0T_{\beta}^0 + (\mathcal{D}^1f)T_{\alpha\beta}^0, \\ T_{\alpha\beta\gamma}^{\kappa} &= (\mathcal{D}^3f)T_{\alpha}^0T_{\beta}^0T_{\gamma}^0 + (\mathcal{D}^2f)[T_{\alpha\beta}^0T_{\gamma}^0 + T_{\alpha\gamma}^0T_{\beta}^0 + T_{\beta\gamma}^0T_{\alpha}^0] \\ &\quad + (\mathcal{D}^1f)T_{\alpha\beta\gamma}^0, \\ T_{\alpha\beta\gamma\delta}^{\kappa} &= (\mathcal{D}^4f)T_{\alpha}^0T_{\beta}^0T_{\gamma}^0T_{\delta}^0 \\ &\quad + (\mathcal{D}^3f)[T_{\alpha\beta}^0T_{\gamma}^0T_{\delta}^0 + T_{\beta\gamma}^0T_{\alpha}^0T_{\delta}^0 + T_{\alpha\delta}^0T_{\beta}^0T_{\gamma}^0 \\ &\quad + T_{\beta\delta}^0T_{\alpha}^0T_{\gamma}^0 + T_{\alpha\gamma}^0T_{\beta}^0T_{\delta}^0 + T_{\gamma\delta}^0T_{\alpha}^0T_{\beta}^0] \\ &\quad + (\mathcal{D}^2f)[T_{\alpha\beta\gamma}^0T_{\delta}^0 + T_{\alpha\beta\delta}^0T_{\gamma}^0 + T_{\alpha\gamma\delta}^0T_{\beta}^0 + T_{\beta\gamma\delta}^0T_{\alpha}^0 \\ &\quad + T_{\alpha\beta}^0T_{\gamma\delta}^0 + T_{\alpha\gamma}^0T_{\beta\delta}^0 + T_{\alpha\delta}^0T_{\beta\gamma}^0] + (\mathcal{D}^1f)T_{\alpha\beta\gamma\delta}^0, \end{aligned} \quad (\text{A } 2)$$

where the coefficients  $\{\mathcal{D}^n f\}$  are functions solely of distance, given by

$$\begin{aligned} \mathcal{D}^1f &= (1 + \kappa r)e^{-\kappa r}, \\ \mathcal{D}^2f &= \kappa^2 r^3 e^{-\kappa r}, \\ \mathcal{D}^3f &= \kappa^2 r^4 (\kappa r - 3)e^{-\kappa r}, \\ \mathcal{D}^4f &= \kappa^2 r^5 (12 - 8\kappa r + \kappa^2 r^2)e^{-\kappa r}, \end{aligned} \quad (\text{A } 3)$$

and all factors of  $1/4\pi\epsilon_0\epsilon$  and, more significantly, every angular dependence of the interaction are embodied in

the bare Coulomb tensors  $T_{\alpha\beta\dots}^0$ , expressions for which are easily calculated.

## Appendix B

### Evaluation of interaction energies

The interaction energy between two discs (A and B), separated by a distance  $r_{AB}$  and oriented at spherical polar angles  $(\theta_A, \phi_A)$  and  $(\theta_B, \phi_B)$  may be written (equation (21)), as a sum of contributions to the total from the interactions of each order of multipole via

$$V_{AB}(r_{AB}, \theta_A, \theta_B, \phi_A, \phi_B) = V_{AB}^{ZZ} + (V_{AB}^{ZQ} + V_{AB}^{QZ}) + V_{AB}^{QQ} \\ + (V_{AB}^{Z\Phi} + V_{AB}^{\Phi Z}) + \dots, \quad (\text{B } 1)$$

where  $Z, Q$  and  $\Phi$  denote, respectively, the charge, quadrupole moment and hexadecapole moment on a disc, and  $V_{AB}^{QZ}$  for instance denotes the contribution from the interaction of the charge on disc A with the quadrupole on disc B.

The leading term in this expansion is simply the screened Coulomb interaction of the two charges, given by

$$V_{AB}^{ZZ} = Z^A e T^\kappa Z^B e = \frac{Z^2 e^2 e^{-\kappa r}}{4\pi\epsilon_0\epsilon r} \quad (\text{B } 2)$$

where  $T^\kappa$  is the zero-order interaction tensor. The next term in equation (B 1) corresponds to the charge–quadrupole interaction,  $V_{AB}^{ZQ}$ , which is written in the following form:

$$V_{AB}^{ZQ} = \frac{e^2}{2!} Z^A T_{\alpha\beta}^\kappa Q_{\alpha\beta}^B. \quad (\text{B } 3)$$

Expressing the screened interaction tensor  $T_{\alpha\beta}^\kappa$  in terms of the unscreened tensors  $\{T_{\alpha\beta\dots}^0\}$ , using equation (A 2), and recalling the definition of the quadrupole moment tensor, equation (13), this sum is calculated via

$$T_{\alpha\beta}^\kappa Q_{\alpha\beta}^B = -Q[\mathcal{D}^2 f T_\alpha^0 T_\beta^0 + \mathcal{D}^1 f T_{\alpha\beta}^0][\delta_{\alpha\beta} - n_\alpha^B n_\beta^B] \\ = -Q\{\mathcal{D}^2 f [T_\alpha^0 T_\alpha^0 - T_\alpha^0 n_\alpha^B T_\beta^0 n_\beta^B] \\ + \mathcal{D}^1 f [T_{\alpha\alpha}^0 - n_\alpha^B T_{\alpha\beta}^0 n_\beta^B]\} \\ = -\frac{Q}{4\pi\epsilon_0\epsilon} \left[ \mathcal{D}^2 f \left( \frac{1 - \cos^2 \theta_B}{r^4} \right) \\ + \mathcal{D}^1 f \left( \frac{1 - 3 \cos^2 \theta_B}{r^3} \right) \right] \\ = \frac{Z a^2}{4} \frac{1}{4\pi\epsilon_0\epsilon} \frac{e^{-\kappa r}}{r^3} [(1 + \kappa r + \kappa^2 r^2) \\ - \cos^2 \theta_B (3 + 3\kappa r + \kappa^2 r^2)], \quad (\text{B } 4)$$

where  $\{n_\alpha^B\}$  denote the Cartesian components of the unit vector which defines the major axis of disc B, and the  $\{\mathcal{D}^n f\}$  are defined by equation (A 3). Along with this energy, the contribution due to the interaction between quadrupole on disc A and charge on disc B must be added. When all multiplicative factors have been included the final result reads:

$$V_{AB}^{ZQ+QZ} \equiv V_{AB}^{ZQ+QZ}(r, \theta_A, \theta_B) \\ = -\frac{Z^2 e^2 a^2}{8} \left( \frac{1}{4\pi\epsilon_0\epsilon} \right) \frac{e^{-\kappa r}}{r^3} \\ \times \left[ \left( 1 + \kappa r + \frac{\kappa^2 r^2}{3} \right) (3 \cos^2 \theta_A + 3 \cos^2 \theta_B) \right. \\ \left. - 2(1 + \kappa r + \kappa^2 r^2) \right], \quad (\text{B } 5)$$

where it is observed that the charge–quadrupole interaction has no dependence on the azimuthal angles  $\phi_A$  and  $\phi_B$ .

In the quadrupole–quadrupole interaction energy it is necessary to calculate the sum  $Q_{\alpha\beta}^A T_{\alpha\beta\gamma\delta}^\kappa Q_{\gamma\delta}^B$ . The screened tensor is expressed as a sum of terms involving the simpler unscreened tensors using equation (A 2), and simplified further by expressing all second and higher rank unscreened tensors in terms of the first-order unscreened tensors, via

$$4\pi\epsilon_0\epsilon T_\alpha^0 = -\frac{r_\alpha}{r^3}, \\ 4\pi\epsilon_0\epsilon T_{\alpha\beta}^0 = \frac{3r_\alpha r_\beta - r^2 \delta_{\alpha\beta}}{r^5} \equiv r \left[ 3T_\alpha^0 T_\beta^0 - \frac{\delta_{\alpha\beta}}{r^4} \right] \\ 4\pi\epsilon_0\epsilon T_{\alpha\beta\gamma}^0 \equiv 15r T_\alpha^0 T_\beta^0 T_\gamma^0 - \frac{3}{r^2} (T_\alpha^0 \delta_{\beta\gamma} + T_\beta^0 \delta_{\alpha\gamma} + T_\gamma^0 \delta_{\alpha\beta}). \quad (\text{B } 6)$$

Following this procedure of expressing the elements of the  $n$ th-rank unscreened tensors in terms of those of the 1st rank tensors, the full unscreened 4th rank tensor, using equations (A 2) and (B 6), is given by

$$T_{\alpha\beta\gamma\delta}^\kappa = T_\alpha^0 T_\beta^0 T_\gamma^0 T_\delta^0 [\mathcal{D}^4 f + 18r \mathcal{D}^3 f + 87r^2 \mathcal{D}^2 f] \\ + [T_\alpha^0 T_\beta^0 \delta_{\gamma\delta} + T_\alpha^0 T_\gamma^0 \delta_{\beta\delta} + T_\alpha^0 T_\delta^0 \delta_{\beta\gamma} + T_\beta^0 T_\gamma^0 \delta_{\alpha\delta} \\ + T_\beta^0 T_\delta^0 \delta_{\alpha\gamma} + T_\gamma^0 T_\delta^0 \delta_{\alpha\beta}] \\ \times [-(\mathcal{D}^3 f / r^3) - 9(\mathcal{D}^2 f / r^2)] \\ + [\delta_{\alpha\beta} \delta_{\gamma\delta} + \delta_{\alpha\gamma} \delta_{\beta\delta} + \delta_{\alpha\delta} \delta_{\beta\gamma}] [\mathcal{D}^2 f / r^6] \\ + \mathcal{D} f T_{\alpha\beta\gamma\delta}^0, \quad (\text{B } 7)$$

where the tensor  $T_{\alpha\beta\gamma\delta}^0$  appearing in the last line of equation (B 7) is the only term surviving if  $\kappa = 0$ , corresponding to the purely Coulombic interaction.

The screened Coulombic tensor  $T_{\alpha\beta\gamma\delta}^\kappa$ , given by equation (B 7), is used to calculate both the contribution to the potential away from a single disc due to the hexadecapole moment  $\Psi^\Phi(\mathbf{r})$  and also the quadrupole–quadrupole and charge–hexadecapole energies in the effective pair potential. For illustrative purposes the quadrupole–quadrupole interaction energy will be pursued here, which involves the sum  $Q_{\alpha\beta}^A T_{\alpha\beta\gamma\delta}^\kappa Q_{\gamma\delta}^B$ . Using equation (B 7) it is evident that this sum will itself be the sum of contributions from terms involving  $Q_{\alpha\beta}^A T_\alpha^0 T_\beta^0 T_\gamma^0 T_\delta^0 Q_{\gamma\delta}^B$ ,  $Q_{\alpha\beta}^A T_\alpha^0 T_\beta^0 \delta_{\gamma\delta} Q_{\gamma\delta}^B$  etc. which must each be calculated separately. The first of these is calculated as

$$\begin{aligned} Q_{\alpha\beta}^A T_\alpha^0 T_\beta^0 T_\gamma^0 T_\delta^0 Q_{\gamma\delta}^B &= Q^2 [\delta_{\alpha\beta} - n_\alpha^A n_\beta^A] [T_\alpha^0 T_\beta^0 T_\gamma^0 T_\delta^0] \\ &\quad \times [\delta_{\gamma\delta} - n_\gamma^B n_\delta^B] \\ &= Q^2 [T_\alpha^0 T_\alpha^0 - T_\alpha^0 n_\alpha^A T_\beta^0 n_\beta^A] \\ &\quad \times [T_\gamma^0 T_\gamma^0 - T_\gamma^0 n_\gamma^B T_\delta^0 n_\delta^B] \\ &= \frac{Q^2}{4\pi\epsilon_0\epsilon} \frac{(1 - \cos^2 \theta_A)(1 - \cos^2 \theta_B)}{r^8}. \end{aligned} \quad (\text{B } 8)$$

Proceeding along these lines for each of the terms appearing in  $Q_{\alpha\beta}^A T_{\alpha\beta\gamma\delta}^\kappa Q_{\gamma\delta}^B$ , the interaction energy finally reads:

$$\begin{aligned} V_{AB}^{QQ} &\equiv \frac{e^2}{2!2!} Q_{\alpha\beta}^A T_{\alpha\beta\gamma\delta}^\kappa Q_{\gamma\delta}^B \\ &= \frac{Z^2 e^2 a^4}{64} (\delta_{\alpha\beta} - n_\alpha^A n_\beta^A) T_{\alpha\beta\gamma\delta}^\kappa (\delta_{\gamma\delta} - n_\gamma^B n_\delta^B) \\ &= \frac{Z^2 e^2 a^4}{64} \left( \frac{1}{4\pi\epsilon_0\epsilon} \right) \\ &\quad \times \left\{ [D^4 f + 18rD^3 f + 87r^2 D^2 f] \frac{1}{r^8} (1 - \cos^2 \theta_A) \right. \\ &\quad \times (1 - \cos^2 \theta_B) \\ &\quad \left. - [D^3 f + 9rD^2 f] \frac{1}{r^7} [8 - 6 \cos^2 \theta_A - 6 \cos^2 \theta_B] \right. \\ &\quad \left. + 4 \cos \theta_A \cos \theta_B (\cos \theta_A \cos \theta_B + \sin \theta_A \sin \theta_B \cos(\Delta\phi)) \right\} \end{aligned}$$

$$\begin{aligned} &+ \frac{D^2 f}{r^6} [6 + 2(\cos \theta_A \cos \theta_B + \sin \theta_A \sin \theta_B \cos(\Delta\phi))^2] \\ &+ \frac{Df}{r^5} [3 - 15 \cos^2 \theta_A - 15 \cos^2 \theta_B - 45 \cos^2 \theta_A \cos^2 \theta_B \\ &+ 6(4 \cos \theta_A \cos \theta_B - \sin \theta_A \sin \theta_B \cos(\Delta\phi))^2] \Big\}, \quad (\text{B } 9) \end{aligned}$$

where attention may be drawn to the fact that the interaction energy involves only the difference in the azimuthal angles,  $\Delta\phi = \phi_A - \phi_B$  and not on their absolute values.

## References

- [1] VERWEY, E. J. W., and OVERBEEK, J. T. G., 1948, *Theory of the Stability of Lyophobic Colloids* (Amsterdam: Elsevier).
- [2] ARORA, A. K., and TATA, B. V. R., 1996, *Ordering and Phase Transitions in Charged Colloids* (New York: VCH).
- [3] VAN ROIJ, R., DIJKSTRA, M., and HANSEN, J. P., 1999, *Phys. Rev. E*, **59**, 2010; VAN ROIJ, R., and HANSEN, J. P., 1997, *Phys. Rev. Lett.*, **79**, 3082.
- [4] VAN OLPHEN, H., 1977, *An Introduction to Clay Colloid Chemistry* (New York: Wiley).
- [5] RAMSAY, J. D. F., and LINDNER, P., 1993, *J. chem. Soc. Faraday Trans.*, **89**, 4207.
- [6] MOURCHID, A., DELVILLE, A., LAMBARD, J., LÉCOLIER, E., and LEVITZ, P., 1995, *Langmuir*, **11**, 1942.
- [7] PIGNON, F. MAGNIN, A., PIAU, J. M., CABANE, B., LINDNER, P., and DIAT, O., 1997, *Phys. Rev. E*, **56**, 3281.
- [8] KROON, M., VOS, W. L., and WEGDAM, G. H., 1998, *Phys. Rev. E*, **57**, 1962.
- [9] BONN, D., KELLAY, H., TANAKA, H., WEGDAM, G. H., and MEUNIER, J., 1999, *Langmuir*, **15**, 7534.
- [10] DIJKSTRA, M., HANSEN, J. P., and MADDEN, P. A., 1997, *Phys. Rev. E*, **55**, 3044.
- [11] KÜTTER, S., HANSEN, J. P., SPRIK, M., and BOEK, E., 2000, *J. chem. Phys.*, **112**, 311.
- [12] TRIZAC, E., and HANSEN, J. P., 1997, *Phys. Rev. E*, **56**, 3137.
- [13] DE CARVALHO, R. J. F., TRIZAC, E., and HANSEN, J. P., 2000, *Phys. Rev. E*, **61**, 1634.
- [14] LÖWEN, H., 1994, *J. chem. Phys.*, **100**, 6738.
- [15] LÖWEN, H., HANSEN, J. P., and MADDEN, P. A., 1993, *J. chem. Phys.*, **98**, 3275.
- [16] HANSEN, J. P., and TRIZAC, E., 1997, *Physica A*, **235**, 257.
- [17] See e.g., JACKSON, J. D., 1999, *Classical Electrodynamics*, 3rd. Edn (New York: Wiley).
- [18] GRIMSON, M. J., and SILBERT, M., 1991, *Molec. Phys.*, **74**, 397.
- [19] VAN ROIJ, R., and EVANS, R., 1999, *J. Phys. Condens. Matter*, **11**, 10047.